NMR and Molecular Modelling Studies on the Solution Structure of the In^{III}–Bleomycin A2 Complex

Athanasios Papakyriakou[a] and Nikos Katsaros*[a]

Keywords: Antitumor agents / Indium / Molecular dynamics / N ligands / NMR spectroscopy

The solution structure of the In^{III}–bleomycin A2 complex (InBLM) has been determined by NMR studies in combination with molecular modelling. Our data indicate that BLM is coordinated to In^{III} through five nitrogen ligands in a distorted tetragonal pyramid configuration. The stability and homogeneity of InBLM has allowed us to obtain a well-defined model of the complex formed at low pH, which is a very potent tumour-imaging agent.

Introduction

The bleomycins (BLMs) are a family of natural antibiotics, exhibiting activity against a broad spectrum of neoplasias.[1,2] Umezawa and co-workers were the first to isolate and characterize BLMs, as their copper chelates, from the culture medium of Streptomyces verticillus.[3,4] The clinically administered drug (Blenoxane or Bleocin) consists predominantly of BLM A2 (55−70%) and BLM B2 in their apo forms (Scheme 1). Their cytotoxicities were recognized to be dependent on the reaction between the ferrous BLM complex and O_2 to produce [HOO−Fe^{III}−BLM], which mediates DNA single- and double-strand scissions.[5−7] Because the biologically active species, designated as "activated bleomycin", is short-lived and unsuitable for direct structural studies, several other metallo-BLMs have been employed as models.[8,9]

The glycopeptide-derived BLM molecule can be divided into four functional domains:

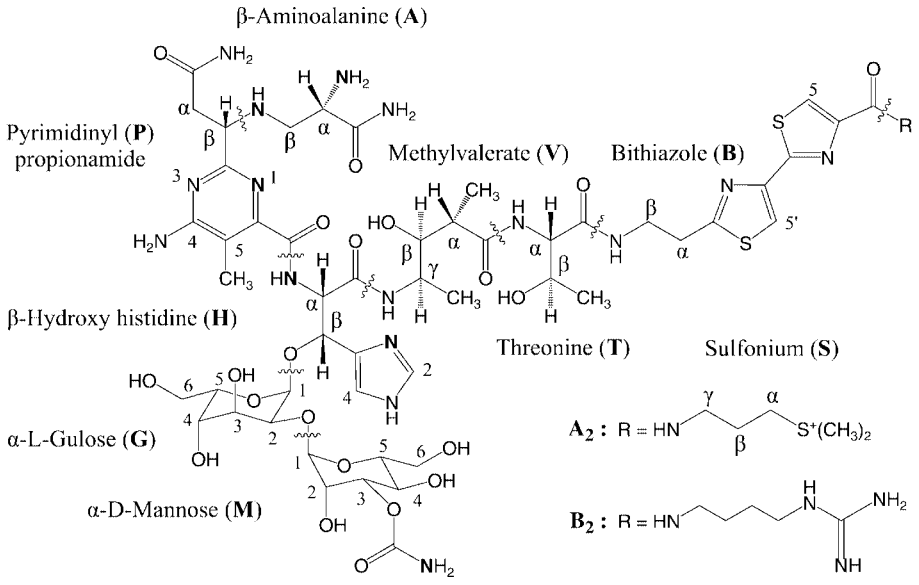

Scheme 1. Structure of bleomycin (BLM) A2 and B2; wavy lines separate their functional domains, and atoms in bold are the proposed N ligands

[a] Institute of Physical Chemistry, NCSR "Demokritos"
15310 Ag. Paraskevi Attikis, Greece
Fax: (internat.) + 30-210/6511766
E-mail: katsaros@chem.demokritos.gr
Supporting information for this article is available on the WWW under http://www.eurjic.org or from the author.

i. the metal-binding domain, made up of β-aminoalanine (**A**), pyrimidinyl propionamide (**P**) and β-hydroxy histidine (**H**)

ii. the linker domain: methyl valerate (**V**) and threonine (**T**)

iii. the DNA-binding domain, with the bithiazole moiety (**B**) intercalating mainly between G-Py base pairs and the sulfonium tail (**S**), different in each BLM

iv. the disaccharide moiety, made up of α-L-gulose (**G**) and 3-*O*-carbamoyl-α-D-mannose (**M**) and considered to be responsible for the sequence specificity of DNA recognition exhibited by the metallo-BLMs.

The equatorial planes of all the metallo-BLMs and analogues studied so far are defined by the secondary amine of **A**, the N1 of pyrimidine, the deprotonated amide of **H** and the N1 of imidazole (Scheme 1).[10−33] In most of these cases, the primary amine of **A** is an axial ligand, as is also the case in the X-ray crystal structure of Cu^{II}−BLM bound to a BLM-binding protein.[18] On the other hand, some NMR studies have introduced a controversy regarding the coordination of the **M** carbamoyl group.[19,26,31,32] Recent conformational analysis of all the binding geometries of Co^{III}−BLMs has been used to explore the configurations available in the proposed binding geometries.[34,35]

A large number of radioactive metal ion complexes of BLM have been prepared and tested as tumour imaging agents.[36−38] Most of them have failed because of a lack either of in vivo stability or of tumour affinity. Among the divalent metal cations of copper, nickel, zinc and cobalt to have demonstrated high affinity for BLM, ^{57}Co−BLM has been clinically used in lung cancer patients and exhibited high specificity. Because of the high toxicity and the inconveniently long half-life of ^{57}Co, other metals such as ^{67}Ga, ^{99m}Tc and ^{111}In have also been introduced as radiolabels. The complex formed at low pH values between ^{111}In and BLM has exhibited a remarkable stability in vivo, since it has no affinity for transferrin.[39−41] In clinical trials, ^{111}InBLM has demonstrated excellent specificity and sensitivity in head and neck cancer.[42−45]

With the aim of obtaining additional structural information for metallo-BLMs, we have undertaken the characterization of the In^{III}−BLM complex in aqueous solutions. Its high stability at low pH values has allowed us to obtain a wealth of information from 2D NMR experiments. The detection of all exchangeable amine and amide protons, especially those of the **A** primary amine, has played the key role in its structure determination. A molecular mechanics force field, specially parameterised for InBLM, was employed in combination with the experimentally obtained results in order to define the chirality of the complex formed. Structural implications and comparison with other metallo-BLMs are discussed.

Results and Discussion

The interaction between In^{III} and BLMs was monitored by ^{1}H NMR spectroscopy, with use being made both of the clinically administered form and of the pure BLM A2. Immediately after the addition of $In(NO_3)_3$ to solutions of the BLMs at room temperature, pH decreases from 4.5 to less than 2.5 were observed, a fact indicating release of protons. The reaction rate is quite high, so formation of InBLM had been completed by the time that the spectra were acquired (ca. 10 min). 1D NMR spectra of InBLM were acquired at a broad range of temperatures from 278 to 333 K, and at pH values ranging from 2.5 to 7.8. The complex demonstrated high stability even after several months at 298 K, equally well in acidic and in neutral solutions. Although 2D NMR experiments were performed at pH = 6.8 and 3.3, only the latter are presented here. Apart from the successful use of the complex formed at the lower pH as a tumour imaging agent, NMR experiments were also better resolved. In particular, the NOESY spectra acquired in H_2O at 278 K exhibited more intense signals, as the exchange and molecular tumbling rates were lower.

Assignment of the NMR Spectra

The ^{1}H and ^{13}C chemical shifts of InBLM are presented in the Supporting Information (Tables S1 and S2), in comparison with those obtained for the metal-free BLM.[19] The ^{1}H chemical shifts of the sugar moieties were assigned by complementary use of ^{1}H−^{13}C heteronuclear and homonuclear experiments. The HMQC experiment (Supporting Information; Figure S1) provides a dispersion in the carbon dimension, sufficient to spread out all the disaccharide H−C cross-peaks. In combination with the long-range couplings observed in the HMBC and TOCSY spectra, complete assignment can be carried out. The strategy for the assignment of the non-exchangeable protons has already been described in detail,[19,25−27] so we present only the assignment procedure for the exchangeable amine and amide protons, which in some cases have proved to be ambiguous.

The amide protons **V**−NH, **T**−NH, **B**−NH and **S**−NH, as well as the secondary amine proton **A**−NH, were readily assigned by observation of their vicinal scalar couplings. No resonance for the amide proton of histidine was detected, as in cases of previously studied metallo-BLMs.[19,20,25−27] This strongly suggests that this amide is deprotonated and coordinated to In^{III}. Four additional pairs of exchangeable protons, strongly coupled to each other, were detected, along with a broad singlet. The first pair of exchangeable protons with signals at δ = 3.57/5.42 ppm was assigned to the primary amine of **A**, due to the detected scalar couplings with **A**−CαH. Moreover, the δ = 5.42 ppm signal exhibits a weak cross-peak to **A**−CβH in the DQF-COSY spectrum, with a ^4J coupling implying that the bonds linking the coupled nuclei are in a sterically fixed "W" configuration (Supporting Information: Figure S2). The next pair of protons, with chemical shifts at δ = 7.13/7.90 ppm, was assigned to **P**−$CONH_2$, due to the weak couplings observed between the δ = 7.90 ppm signal and the two **P**−Cα protons, also supported by the observed NOEs (Supporting Information: Figure S3). The set of coupled protons at δ = 7.68/8.40 ppm was assigned to **A**−$CONH_2$, by virtue of the scalar coupling between the δ = 8.40 ppm signal and **A**−CαH. This ^4J coupling is also quite weak and its detection indicates a fixed conformation between the coupled nuclei. The broad signal at δ = 7.31 ppm was assigned to 4-

NH_2 of the pyrimidine ring, in view of the medium-sized NOE exhibited with the neighbouring **P**−5-CH_3. The last pair of protons at δ = 5.96/6.63 ppm exhibits only quite weak NOEs with **P**−5-CH_3 and was assigned to the remaining **M**−$CONH_2$ group. This was also the case for Ga^{III}−BLM, while their chemical shift values are also comparable.

Analysis of the NMR Data

Detection and assignment of the exchangeable protons has revealed very important information regarding the structure of InBLM. The degeneration of the **A**−αNH_2 resonance at δ = 3.57 and 5.42 ppm is a strong indication of its coordination to the metal ion. In the opposite case, only one signal would be detected for the equivalent amine protons, due to fast rotation around the Cα−N bond. In contrast, the potential carbamoyl N ligand of **M** is disfavoured by the fact that it should be deprotonated, the histidine amide likewise. Owing to the high pK_a of **M**−NH_2 (ca. 13) and the detection of two proton resonances, **M**−CO is thus more likely to be a ligand.[46]

A wealth of structural data and distance constraints has been obtained from NOESY spectra acquired at low temperature (278 K; Supporting Information: Table S3). The observed NOEs between the protons of **H**, **V** and **T** suggest that the linker domain is folded underneath the equatorial plane from the side of the imidazole, in the same way as for the Cu^{II}, Co^{III} and Ga^{III}−BLMs.[18,25,27,33] The thiazolium rings are probably in a *trans* conformation, since through-space coupling between their aromatic protons is absent. On the other hand, **B**−5′H exhibits NOEs with the methyl groups of **V**, indicating that the bithiazole tail is close to the linker domain.

Probably the most interesting piece of information is the observation of NOEs between **A**−αNH_2 and the disaccharide protons. Medium-sized signals with **M**−C3H and **M**−C2 H, as well as weak ones with **M**−C1H and **G**−C5 H, restrain the aminoalanine moiety near the sugars. Consequently, it would be expected that both **A** and **M** moieties should share the same side of the equatorial plane. The existence only of one weak NOE between **M**−NH_2 and **P**−CH_3 points to the stacking of the carbamoyl group over the **P** ring, just as in Cu^{II}, Co^{III} and Ga^{III}−BLMs.[18,25,27,33]

Molecular Dynamics Calculations

Three different models of InBLM were used as starting structures for restrained simulated annealing calculations (Figure 1). These models were constructed with In^{III} bound to the four common N ligands of most metallo-BLMs studied so far. Only four-coordinate species were used, so as to make a direct comparison between their potential energies. Model **I** was constructed with both **A**−αNH_2 and **M**−$CONH_2$ at the same side of the equatorial plane, while in models **II** and **III** they occupy apical positions across the equatorial plane. In this way, we were able to examine whether **A**−αNH_2 and **M**−$CONH_2$ are potential axial ligands for InBLM. The coordinates of model **I** were based on the crystal structure of Cu^{II}−BLM (PDB accession no. 1JIF)[18] and models **II** and **III** were constructed on the basis of the NMR structure of Co^{II}−BLM (PDB accession no. 1DEY).[31]

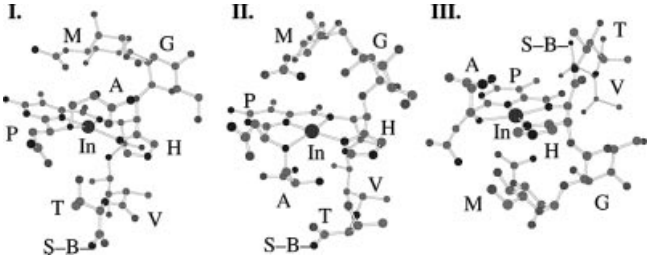

Figure 1. Starting four-coordinate models of InBLM employed in the molecular dynamics calculations; the equatorial ligands are similar in all structures, while the **A** primary amine and the **M** carbamoyl group are located at different sites: both at the same side of the equatorial plane (**I**) and each one occupying an axial position (**II** and **III**); hydrogen atoms, bithiazole and sulfonium moieties have been excluded for clarity

The results obtained by the 10 best structures, by virtue of the lowest potential energies and deviations from the NMR constraints, are summarized in Table 1. All the starting models resulted in structures with the aminoalanine and the disaccharide moieties on the same side of the equatorial plane (Supporting Information: Figure S3). In addition to

Table 1. Structural and energy statistics of the InBLM best models obtained from the simulated annealing calculations

	Structure **I**	Structure **II**	Structure **III**
Rmsd of heavy atoms [Å]	0.90 ± 0.23	0.98 ± 0.19	1.64 ± 0.37
Rmsd from distance restraints [Å]	0.019 ± 0.001	0.022 ± 0.002	0.044 ± 0.002
No. of distance restraint violations	3−5	4−7	11−16
Potential energy terms [kcal mol^{-1}]:			
Total	−28.7 ± 4.1	−18.5 ± 1.5	58.2 ± 3.6
Bond	22.5 ± 0.9	23.4 ± 1.0	25.5 ± 0.8
Angle	56.8 ± 1.2	63.2 ± 1.8	86.6 ± 6.4
Dihedral angle[a]	42.0 ± 1.6	43.7 ± 1.5	55.2 ± 2.6
Nonbonded[b]	−151.9 ± 7.0	−151.1 ± 3.7	−118.2 ± 8.9
Constraint	2.0 ± 0.1	2.2 ± 0.4	8.9 ± 0.8

[a] Including the improper angle energy term. [b] Sum of the electrostatic and van der Waals energy terms.

this, structures resulting from model **I** exhibit lower energies and deviations from the distance constraints. Model **I** with **A**−αNH$_2$ and **M**−CONH$_2$ on the same side of the equatorial plane is therefore strongly favoured.

Coordination of **A**−αNH$_2$ is supported not only by the NMR spectroscopic data, but also by the molecular dynamics results. In most of the final structures, especially those resulting from models **I** and **II**, the primary amine is to be found at the axial site, while the carbamoyl group is stacked over the pyrimidine ring. Even though the calculated distance between In^{III} and the **A** amine nitrogen (ca. 2.9 Å) cannot be regarded as a metal−ligand bond length, it is evident that **A**−αNH$_2$ is a favoured axial ligand. The distance between the **M** carbamoyl oxygen atom and In^{III} is > 4.5 Å in all the final structures and can thus be discounted as ligand.

The average structure of the 10 best models **I** was subjected to energy minimization, but with **A**−αNH$_2$ bonded to In^{III}. All the experimental constraints were applied with no violation > 0.1 Å and the total energy was calculated to be even lower than those of the four-coordinate models. The resulting structure, as illustrated in Figure 2, represents the favourable solution structure of InBLM. On the basis of the higher thermodynamic and in vivo stabilities of the six-coordinate In^{III} complexes,[47] we can hypothesize that an H_2O molecule or a Cl^- ion might occupy an axial site *trans* to the primary amine ligand.

Structural Implications and Comparisons with Other Metallo-BLMs

An examination of InBLM structure (Figure 2) has revealed potential H bonds between different domains of BLM. A very strong one is exhibited by (**T**)O−H···O=C(**P**) (distance 1.7 Å, angle 166°). Moreover, the hydroxy oxygen atom of **T** can act as an acceptor to **A**−NH (distance 1.9 Å, angle 170°). These two H bonds, along with those between **T**−NH, **V**−NH and the potential sixth exogenous ligand (H_2O or Cl^-), might be responsible for the folded conformation of the linker domain. The result of electron shielding by the imidazole ring current is exhibited by the upfield-shifted resonances of valerate.

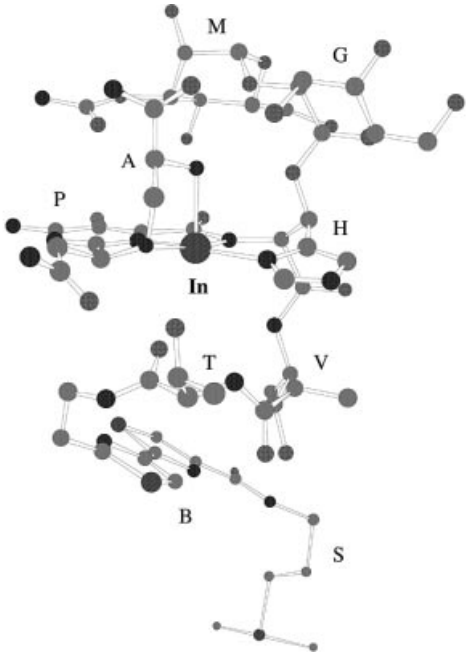

Figure 2. Favoured model for the solution structure of InBLM with the primary amine of aminoalanine occupying the axial site; this model was calculated by averaging of the coordinates of the 10 best models **I** and energy minimization with all the distance restraints

Some potential H bonds were also observed at the other side of the InBLM equatorial plane: (**M**)O4−H···O=C(**H**) (distance 1.7 Å, angle 175°), (**G**)O3−H···O=C(**A**) (distance 1.8 Å, angle 161°), (**A**)αN−H···O−C3(**G**) (distance 2.1 Å, angle 154°) and the weak (**A**)αN−H′···O=C3(**M**) (distance 2.7 Å, angle 116°). These interactions may account for an approach of the disaccharide moiety towards the axial amine ligand, which was also observed in the crystal structure of Cu^{II}−BLM,[18] as well as in the solution structures of Co^{III} and Ga^{III}−BLMs.[25,27,33] A noticeable difference between the structures of these metallo-BLMs is the location of the DNA-binding domain. While for CoBLM ("brown form") and GaBLM no NOEs were detected between **B** or **S** and any other moieties, the NMR structures of CoBLM ("green form") and InBLM have revealed some sort of folding for the BLM's tail. Since no interactions such as the H bonds mentioned above were found, we cannot provide an explanation for this variation.

Conclusion

The anticancer drug BLM forms a very stable complex with In^{III} at low pH values. Our NMR spectroscopic data indicate that InBLM is also stable at neutral pH for several months. The five N ligands of BLM form a distorted tetragonal pyramid around the metal cation, as in the case of Cu^{II}−BLM crystal structure. The carbamoyl group of mannose is not a ligand, but is constrained to the second coordination sphere of InBLM through H-bonding interactions with the axial amine ligand.

Experimental Section

Sample Preparation: Bleocin and BLM A2 were a kind gift from Nippon Kayaku Co. and were used without further purification. The complex was prepared at room temperature by addition of In(NO$_3$)$_3$·3H$_2$O (0.1 M) to aqueous solutions of BLM (10 mM) and the pH was adjusted with aliquots of dilute NaOD or DCl. For the NMR experiments, lyophilised samples were dissolved either in 90% H_2O/10% D_2O or in D_2O (99.99%) (final concentrations were 3−5 mM). The purity of InBLM was judged to be $> 95\%$ from the ^{1}H NMR spectra. All the samples were stable over a period of several months at room temperature, since no changes were detected in their periodically recorded ^{1}H NMR spectra .

NMR Experiments: NMR spectra were recorded with a Bruker Avance 500 MHz instrument and were processed by X-WIN NMR 2.6 (Bruker Analytik GmbH). The program SPARKY 3.100,[48] running on a Linux PC, was used for assignment and analysis of

the 2D spectra. ^1H and ^{13}C chemical shifts were referenced to sulfonium tail methyl groups of BLM at $\delta = 2.93$ and 25.0 ppm, respectively. 2D NOESY (100, 200 and 400 ms mixing times), DQF COSY[49] and TOCSY experiments (MLEV-17 sequence with 35 and 70 ms mixing times)[50] were recorded at 278 and 298 K in H_2O and D_2O. Data sets with 4096 × 512 complex points were acquired with 7 kHz sweep widths in both dimensions and 32 scans per t_1 increment. $^1H-^{13}C$ HMQC[51] and HMBC[52] experiments were also recorded at 278 and 298 K in H_2O and D_2O. Data sets with 2048 × 256 points were collected with 32 or 64 scans per t_1 increment and spectral widths of 6 kHz in the proton and 25 kHz in the carbon dimension. Solvent suppression for the H_2O samples was performed by use of excitation sculpting with gradients,[53] while for the D_2O samples a presaturation pulse was used during the relaxation delay of 2.0 s. The indirect dimension was zero-filled to 2048 data points and the FIDs were processed either with a combination of exponential and Gaussian weighting functions or with a 90°-shifted sine bell function.

Distance Constraints: The NOE signals from the 200-ms NOESY spectrum of InBLM at pH = 3.3 and 278 K were classified as strong, medium and weak, by visual inspection of the cross-peak intensities. Integration of the cross-peaks was performed by the sum-over-ellipse method. The constraints were set to upper distance limits of 3.0, 4.0 and 5.0 Å, respectively, while an additional 1.0 Å was allowed for NOEs involving methyl groups and ambiguous methylene protons. A total of 88 distance constraints were applied with a 50 kcal mol^{-1} $Å^{-2}$ force constant, by use of a square bottom well function with parabolic sides out to 0.5 Å and then linear sides beyond that.

Force Field Parameters: All the molecular modelling calculations were performed with Amber 6,[54] running on a Linux PC. In order to model InBLM accurately, the Amber-1994 force field was modified according to the guidelines of its authors.[55] Standard atom types were assigned to the atoms of BLM by analogy to their chemical environment, except for the disaccharide moiety, for which we used parameters from a force field for modelling glycoproteins (GLYCAM).[56] A new atom type was created for In^{III}, with van der Waals parameters estimated as $R^* = 1.9$ Å (from Bondi crystallographic data)[57] and $\varepsilon = 0.2$ kcal mol^{-1}. The bond, angle and dihedral angle parameters of BLM were also chosen among the existing Amber force field parameter, on the basis of atom type analogy. The metal−ligand parameters were adapted from those calculated by Welch et al.[58] Bond lengths of In−N were applied with $R_o = 2.38$ Å and a 50 kcal mol^{-1} $Å^{-2}$ force constant. For the N−In−N angles we applied θ_o of 90 or 180° with 50 kcal mol^{-1} rad^{-2} force constant, while dihedral angles involving In^{III} were set with zero force constants. The atom-centred point charges of the complex were generated from the electrostatic potential of its molecular fragments. For this purpose, we used the ab initio program package GAMESS,[59] at the Hartree-Fock level of theory. The Stevens/Basch/Krauss/Jasien/Cundari-21G relativistic effective core potentials (SBKJC VDZ ECPs)[60] were used for indium, the 6-31G* basis set for all other atoms.[61] The point charges were fitted to reproduce the electrostatic potential by use of the RESP method,[62] a two-stage approach in which the equivalent methyl and methylene hydrogen atoms are restrained to have the same charge. The equatorial plane of InBLM comprising the β-aminoalanine, pyrimidinylpropionamide and histidine moieties was fitted as a whole. For the remaining domains of BLM we used the atom charges, previously calculated for GaBLM.[33]

Restrained Molecular Dynamics: Molecular dynamics calculations in vacuo were carried out at a time step of 1 fs with the Amber distance-dependent dielectric constant algorithm. The cut-off distance was set to 16.0 Å and the nonbonded pair list was updated every 10 steps. Temperature regulation was performed by use of the Berendsen algorithm. For the heating and cooling stages a bath coupling constant of 0.1−0.5 ps was applied, so as to assure a tighter coupling to the heat bath, while for the equilibration stages it was increased to 2.0 ps to allow sampling of more natural trajectories. The simulated annealing procedure used is the same as that described in the structural characterization of GaBLM.[33] Starting models were initially energy-minimized with no restraints by 500 steps of the steepest descent method and followed by the conjugate gradient method to an rms gradient < 0.1. Every model was then subjected to 20 individual runs starting with a different seed for the initial velocities assigned. A final structure from each iteration was generated by mass-weighted rms fitting and averaging of the coordinates from the last 20 ps of the trajectory (100 structures), followed by energy minimization as above but with all the restraints applied. The results presented in Table 1 are derived from the final 10 best models, by virtue of the lowest energy and deviations from the NMR constraints.

Supporting Information (see footnote on the first page of this article): Two tables with the ^1H and ^{13}C chemical shifts of InBLM in comparison with those reported for apo-BLM and a table with the categorized NOE intensities of InBLM in comparison with those obtained for GaBLM. Three figures with expanded regions from the HMQC, DQF-COSY and NOESY spectra of InBLM and a figure with ensembles of the superimposed structures calculated for each starting model.

Acknowledgments

This work was supported by the General Secretariat for Research and Technology of Greece. The authors are grateful to Prof. Ivano Bertini for his hospitality at the CERM in the framework of the European Large Research Infrastructure.

[1] F. Hutchinson, L. F. Povirk in *Bleomycin: Chemical, Biochemical, and Biological Aspects* (Ed.: S. M. Hecht), Springer-Verlag, New York, **1979**, pp. 256−266.
[2] H. Umezawa in *Anticancer Agents Based on Natural Product Models* (Eds.: J. M. Cassady, J. Douros), Academic Press, New York, **1980**, pp. 147−166.
[3] H. Umezawa, K. Maeda, T. Takeuchi, Y. Okami, *J. Antibiot.* **1966**, *19*, 200−209.
[4] H. Umezawa, Y. Suhura, T. Takita, K. Maeda, *J. Antibiot.* **1966**, *19*, 210−219.
[5] S. M. Hecht, *Acc. Chem. Res.* **1986**, *19*, 383−391.
[6] J. Stubbe, J. W. Kozarich, *Chem. Rev.* **1987**, *87*, 1107−1136.
[7] R. M. Burger, *Chem. Rev.* **1998**, *98*, 1153−1169.
[8] C. A. Claussen, E. C. Long, *Chem. Rev.* **1999**, *99*, 2797−2816.
[9] J. Stubbe, J. W. Kozarich, W. Wu, D. E. Vanderwall, *Acc. Chem. Res.* **1996**, *29*, 322−330.
[10] Y. Iitaka, H. Nakamura, T. Nakatani, Y. Muraoka, A. Fujii, T. Takita, H. Umezawa, *J. Antibiot.* **1978**, *31*, 1070−1072.
[11] T. Takita, Y. Muraoka, T. Nakatani, A. Fujii, Y. Iitaka, H. Umezawa, *J. Antibiot.* **1978**, *31*, 1073−1077.
[12] S. J. Brown, P. K. Mascharak, *J. Am. Chem. Soc.* **1988**, *110*, 1996−1997.
[13] S. J. Brown, S. E. Hudson, D. W. Stephan, P. K. Mascharak, *Inorg. Chem.* **1989**, *28*, 468−477.
[14] E. Kimura, H. Kurosaki, Y. Kurogi, M. Shionoya, M. Shiro, *Inorg. Chem.* **1992**, *31*, 4314−4321.
[15] J. D. Tan, S. E. Hudson, S. J. Brown, M. M. Olmstead, P. K. Mascharak, *J. Am. Chem. Soc.* **1992**, *114*, 3841−3853.
[16] H. Kurosaki, K. Hayashi, Y. Ishikawa, M. Goto, K. Inada, I.

Taniguchi, M. Shionoya, E. Kimura, *Inorg. Chem.* **1999**, *38*, 2824−2832.
[17] B. Mouzopoulou, H. Kozlowski, N. Katsaros, A. Garnier-Suillerot, *Inorg. Chem.* **2001**, *40*, 6923−6929.
[18] M. Sugiyama, T. Kumagai, M. Hayashida, M. Maruyama, *J. Biol. Chem.* **2002**, *277*, 2311−2320.
[19] M. A. J. Akkerman, C. A. G. Haasnoot, C. W. Hilbers, *Eur. J. Biochem.* **1988**, *173*, 211−225.
[20] M. A. J. Akkerman, E. W. Neijman, S. S. Wijmenga, C. W. Hilbers, W. Bermel, *J. Am. Chem. Soc.* **1990**, *112*, 7462−7474.
[21] R. X. Xu, W. E. Anthroline, D. H. Petering, *J. Biol. Chem.* **1992**, *267*, 944−949.
[22] R. X. Xu, D. Nettesheim, J. D. Otvos, D. H. Petering, *Biochemistry* **1994**, *33*, 907−916.
[23] W. Wu, D. E. Vanderwall, J. W. Kozarich, J. Stubbe, C. J. Turner, *J. Am. Chem. Soc.* **1994**, *116*, 10843−10844.
[24] W. Wu, Q. Mao, P. Fulmer, W. Li, E. F. DeRose, D. H. Petering, *J. Biol. Chem.* **1996**, *271*, 6185−6191.
[25] W. Wu, D. E. Vanderwall, S. M. Lui, X.-J. Tang, C. J. Turner, J. W. Kozarich, J. Stubbe, *J. Am. Chem. Soc.* **1996**, *118*, 1268−1280.
[26] J. D. Otvos, W. E. Antholine, S. Wehrli, D. H. Petering, *Biochemistry* **1996**, *35*, 1458−1465.
[27] S. M. Lui, D. E. Vanderwall, W. Wu, X.-J. Tang, C. J. Turner, J. W. Kozarich, J. Stubbe, *J. Am. Chem. Soc.* **1997**, *119*, 9603−9613.
[28] J. Caceres−Cortes, H. Sugiyama, K. Ikudome, I. Saito, A. H. Wang, *Eur. J. Biochem.* **1997**, *244*, 818−828.
[29] T. E. Lehmann, L.-J. Ming, M. E. Rosen, L. Jr. Que, *Biochemistry* **1997**, *36*, 2807−2816.
[30] W. Wu, D. E. Vanderwall, S. Teramoto, S. M. Lui, S. T. Hoehn, X.-J. Tang, C. J. Turner, D. L. Boger, J. W. Kozarich, J. Stubbe, *J. Am. Chem. Soc.* **1998**, *120*, 2239−2250.
[31] T. E. Lehmann, M. L. Serrano, L. Jr. Que, *Biochemistry* **2000**, *39*, 3886−3898.
[32] T. E. Lehmann, *J. Biol. Inorg. Chem.* **2002**, *7*, 305−312.
[33] A. Papakyriakou, B. Mouzopoulou, N. Katsaros, *J. Biol. Inorg. Chem.* **2003**, *8*, 549−559.
[34] F. Fedeles, M. Zimmer, *Inorg. Chem.* **2001**, *40*, 1557−1561.
[35] M. Zimmer, *Coord. Chem. Rev.* **2001**, *212*, 133−163.
[36] R. B. Grove, R. C. Reba, W. C. Eckelman, M. Goodyear, *J. Nucl. Med.* **1974**, *15*, 386−390.
[37] E. B. Silberstein, *Am. J. Med.* **1976**, *60*, 226−237.
[38] D. Front, O. Israel, G. Iosilevsky, E. Even-Sapir, A. Frenkel, G. M. Kolodny, M. Feinsod, *J. Nucl. Med.* **1988**, *29*, 187−194.
[39] D. Y. Hou, H. Hoch, G. S. Johnston, K. C. Tsou, R. J. Farkas, E. E. Miller, *Eur. J. Nucl. Med.* **1983**, *8*, 535−540.
[40] D. Y. Hou, H. Hoch, G. S. Johnston, K. C. Tsou, A. E. Jones, R. J. Farkas, E. E. Miller, *J. Surg. Oncol.* **1984**, *25*, 168−175.
[41] D. Y. Hou, H. Hoch, G. S. Johnston, K. C. Tsou, R. J. Farkas, E. E. Miller, *Int. J. Nucl. Med. Biol.* **1984**, *11*, 129−39.
[42] D. A. Goodwin, C. F. Meares, L. H. DeRiemer, C. I. Diamanti, R. L. Goode, J. E. Baumert, Jr., D. J. Sartoris, R. L. Lantieri, H. D. Fawcett, *Nucl. Med.* **1981**, *22*, 787−792.
[43] A. P. Jekunen, K. J. Kairemo, H. A. Ramsay, M. J. Kajanti, *Clin. Nucl. Med.* **1996**, *21*, 129−131.
[44] K. J. Kairemo, H. A. Ramsay, T. Paavonen, S. Bondestam, *Eur. J. Cancer. B. Oral. Oncol.* **1996**, *32*, 311−321.
[45] K. J. Kairemo, H. A. Ramsay, T. K. Paavonen, H. A. Jaaskela-Saari, M. Tagesson, K. Ljunggren, S. E. Strand, *Cancer. Detect. Prev.* **1997**, *21*, 83−90.
[46] R. H. Holm, P. Kennepohl, E. I. Solomon, *Chem. Rev.* **1996**, *96*, 2239−2314.
[47] Y. Sun, C. J. Anderson, T. S. Pajeau, D. E. Reichert, R. D. Hancock, R. J. Motekaitis, A. E. Martell, M. J. Welch, *J. Med. Chem.* **1996**, *39*, 458−470.
[48] T. D. Goddard, D. G. Kneller, *SPARKY 3*, University of California, San Francisco, **2001**.
[49] A. Derome, M. Williamson, *J. Magn. Reson.* **1990**, *88*, 177−185.
[50] A. Bax, D. G. Davis, *J. Magn. Reson.* **1985**, *65*, 355−360.
[51] A. Bax, S. Subramanian, *J. Magn. Reson.* **1986**, *67*, 565−569.
[52] A. Bax, M. F. Summers, *J. Am. Chem. Soc.* **1986**, *108*, 2093−2094.
[53] T.-L. Hwang, A. J. Shaka, *J. Magn. Reson.* **1995**, *112*, 275−279.
[54] D. A. Case, D. A. Pearlman, J. W. Caldwell, T. E. Cheatham, W. S. Ross, C. L. Simmerling, T. A. Darden, K. M. Merz, R. V. Stanton, A. L. Cheng, J. J. Vincent, M. Crowley, V. Tsui, R. J. Radmer, Y. Duan, J. Pitera, I. Massova, G. L. Seibel, U. C. Singh, P. K. Weiner, P. A. Kollman, *AMBER 6*, University of California, San Francisco, **1999**.
[55] W. D. Cornell, P. Cieplak, C. I. Bayly, I. R. Gould, K. M. Jr. Merz, D. M. Ferguson, D. C. Spellmeyer, T. Fox, J. W. Caldwell, P. A. Kollman, *J. Am. Chem. Soc.* **1995**, *117*, 5179−5197.
[56] R. J. Woods, R. A. Dwek, C. J. Edge, B. Fraser-Reid, *J. Phys. Chem.* **1995**, *99*, 3832−3846.
[57] A. Bondi, *J. Phys. Chem.* **1964**, *68*, 441−451.
[58] D. E. Reichert, M. J. Welch, *Coord. Chem. Rev.* **2001**, *212*, 111−131.
[59] M. W. Schmidt, K. K. Baldridge, J. A. Boatz, S. T. Elbert, M. S. Gordon, J. J. Jensen, S. Koseki, N. Matsunaga, K. A. Nguyen, S. Su, T. L. Windus, M. Dupuis, J. A. Montgomery, *J. Comput. Chem.* **1993**, *14*, 1347−1363.
[60] W. J. Stevens, M. Krauss, H. Basch, P. G. Jasien, *Can. J. Chem.* **1992**, *70*, 612.
[61] M. M. Francl, W. J. Pietro, W. J. Hehre, J. S. Binkley, M. S. Gordon, D. J. DeFrees, J. A. Pople, *J. Chem. Phys.* **1982**, *77*, 3654−3665.
[62] C. I. Bayly, P. Cieplak, W. D. Cornell, P. A. Kollman, *J. Phys. Chem.* **1993**, *97*, 10269−10280.

Received February 5, 2003

